Research Square

Preprints are preliminary reports that have not undergone peer review.
They should not be considered conclusive, used to inform clinical practice,
or referenced by the media as validated information.

Seasonal shifts in spatial and temporal beta diversity of diatoms in a Mediterranean lagoon (El Mellah, Algeria)

Mohamed Faouzi SAMAR

samar.moh.faouzi@univ-eltarf.dz

Chadli Bendjedid University

Fatiha BAKARIA

Chadli Bendjedid University

Nedjma LAROUCI

Chadli Bendjedid University

Khadidja Wissal ABDALLAH

Chadli Bendjedid University

Research Article

Keywords: Beta diversity, Diatoms, Mediterranean lagoon, Spatial structure, Environmental gradients

Posted Date: March 25th, 2026

DOI: https://doi.org/10.21203/rs.3.rs-9087545/v1

License: This work is licensed under a Creative Commons Attribution 4.0 International License. Read Full License

Additional Declarations: No competing interests reported.

Abstract

Mediterranean lagoons experience pronounced seasonal forcing and sharp environmental gradients that can generate strong spatiotemporal variability in phytoplankton composition. We investigated seasonal changes in diatom community beta diversity in El Mellah Lagoon (Algeria) based on four field campaigns performed in 2016 at 31 stations spanning littoral and pelagic sectors. Spatial beta diversity within each season was estimated using Jaccard dissimilarity and decomposed into turnover and nestedness components to clarify whether among-station differences were primarily driven by species replacement or richness-related patterns. Temporal change between successive seasons was quantified using the Temporal Beta Index (TBI), separating species losses from gains at the station level. The contribution of individual taxa and sites to overall compositional variability was assessed using SCBD and LCBD indices, and spatial dependence was evaluated using Moran's I and variogram parameters prior to kriging-based mapping. Seasonal typologies were further explored using a Factor Analysis of Mixed Data (FAMD) integrating beta-diversity descriptors with measured environmental variables. Beta-diversity patterns differed strongly among seasons, and temporal transitions showed contrasting loss–gain balances, indicating that seasonal change in composition was not symmetric across the annual cycle. Spatial autocorrelation and variogram ranges varied by season and by beta-diversity component, highlighting shifts between more clustered and more spatially diffuse configurations. A limited set of taxa contributed disproportionately to beta diversity, while several stations emerged as recurrently distinctive assemblages. Overall, these results illustrate how integrating beta-diversity partitioning, contribution metrics and geostatistical analyses can be used to describe seasonal and spatial community change in Mediterranean lagoon systems

Introduction

However, in Mediterranean lagoons, where strong environmental variability co-occurs with multiple human-mediated influences (Bellino et al. 2019; Gálvez et al. 2023), beta-diversity patterns and their drivers remain insufficiently documented.

Biodiversity loss represents one of the most pressing ecological challenges of our time. While traditional studies have predominantly focused on species richness as the primary metric of biodiversity change, recent research has increasingly highlighted the importance of community composition, which varies across both spatial and temporal dimensions (Baselga 2010; Soininen et al. 2017a). Beyond local richness, compositional turnover-or beta diversity-provides a complementary view of biodiversity change and has been increasingly used to describe ecological variation in aquatic ecosystems(Rega et al. 2023; Rolls et al. 2023; Marion et al. 2017; Nakov et al. 2019)

Two principal patterns can characterize beta-diversity change: biotic homogenization, where communities become more similar across time or space, and biotic differentiation, where dissimilarity among communities increases (Rolls et al. 2023; He et al. 2023). Both patterns have been widely reported across ecosystems and are often discussed in relation to environmental change and human disturbance (Carvalho et al. 2012). Yet, most syntheses and large comparative studies have focused on terrestrial ecosystems or large aquatic systems, leaving a gap for small, heterogeneous transitional waters such as Mediterranean

coastal lagoons, where local gradients, hydrodynamics, and human activities interact over short distances (Pitacco et al. 2019) .

The drivers underlying beta-diversity patterns are complex and multifaceted. Recent studies suggest that observed patterns arise from the joint influence of seasonal environmental variability, disturbance regimes (Tatsumi et al. 2020), species dispersal capacity and habitat connectivity (Yao et al. 2024), habitat degradation (Guelu et al. 2024), and biotic interactions (Hammill et al. 2018). In coastal lagoons, these drivers operate simultaneously across multiple temporal scales—from daily hydrodynamic fluctuations to seasonal cycles—creating highly dynamic environmental mosaics (Heilpern 2018). Such mosaics can homogenize communities when conditions converge across sites or, conversely, promote differentiation when spatial gradients and niche contrasts intensify.

Within this context, the El Mellah Lagoon (northeastern Algeria) offers a relevant case study to examine how community composition varies across space and seasons in a Mediterranean lagoon exposed to marked environmental gradients and multiple human-mediated influences. Previous work in El Mellah Lagoon has documented its physicochemical setting and seasonal plankton dynamics (Draredja et Kara 2004 ; Draredja 2007; Draredja et al. 2019) and its sedimentary dinoflagellate cyst assemblages (Draredja et al. 2020). Additional studies have highlighted potential stressors including nutrient enrichment linked to domestic and agricultural inputs, restricted water exchange in semi-enclosed zones, elevated organic matter loads, and localized physical disturbances associated with shoreline activities (Amara et al. 2017; Kherifi et al. 2019; Larouci et al. 2024). Together, these factors contribute to spatial and temporal heterogeneity in environmental conditions that can structure biological communities and shape beta-diversity patterns through turnover and nestedness processes.

Diatoms (Bacillariophyceae) provide a useful biological model for investigating these dynamics. With high species diversity, short generation times, and well-known sensitivity to environmental gradients-including nutrients, salinity, pH, and oxygen availability-diatoms respond rapidly to changing conditions and integrate environmental variation over ecologically relevant timescales (Jamoneau et al. 2017; Wu et al. 2022a). Their taxonomy and ecology are relatively well established, supporting robust community-based analyses in transitional waters. We focused on water-column samples because El Mellah is shallow and frequently mixed, leading to a structurally mixed assemblage that includes planktonic and tychoplanktonic taxa.

This study addresses the central question of how diatom beta diversity reflects spatiotemporal variation in a Mediterranean coastal lagoon characterized by strong seasonality and heterogeneous environmental conditions? We hypothesize that beta-diversity patterns will show spatial differentiation associated with lagoon-scale gradients, with temporal shifts reflecting seasonal changes in environmental conditions. Specifically, we aimed to: (i) characterize the seasonal structuring of diatom community composition across the lagoon, (ii) decompose beta diversity into turnover and nestedness components to identify the dominant mechanisms underlying community differences among stations, and (iii) examine associations between observed beta-diversity patterns and measured environmental variables. In the present study, measured nutrient concentrations and chlorophyll-a were used as proxies of trophic status, allowing diatom community patterns to be interpreted along a quantified eutrophication gradient; however, it adopts a correlative framework and does not directly quantify specific nutrient sources. By addressing these objectives, this work

contributes to improving our understanding of spatiotemporal community variation in Mediterranean transitional waters and provides a basis for interpreting beta-diversity patterns in relation to environmental gradients in coastal lagoons.

Materials and Methods

Study Area

The El Mellah Lagoon is located in northeastern Algeria (36°54' N, 8°20' E) along the Mediterranean coast (Fig. 1). It forms part of El Kala National Park, a protected area recognized for its high ecological diversity and designated as a Ramsar site in 2004.

The lagoon has an elongated ovoid shape, oriented from north-northwest to south-southeast, and covers approximately 865 hectares. It is approximately 4.5 km long and 2.5 km wide. A natural channel, approximately 900 m long, connects the lagoon to the Mediterranean Sea, allowing partial hydrological exchange between marine and lagoonal waters. The depth varies spatially, reaching up to 6 m in the central zone, with steep slopes on the western side. The eastern sector is shallower, rarely exceeding 2 m in the first 500 m before a marked slope break (Guelorget et al. 1982). A dune belt rising to 177 m altitude lies to the northeast, shaping much of the surrounding landscape. The lagoon is bordered by the Mediterranean Sea to the north, El Kala Wildlife Park and Ain Khiar Forest to the south, Boumalek Forest and peri-urban area of El Gantra El Hamara to the east, and the localities of El Mellah and Souk Rguibet to the west.

Sampling Design

This study assessed the ecological status of El Mellah Lagoon using a spatial and temporal beta-diversity framework based on phytoplankton composition, with diatoms considered as the model taxon. Sampling stations were randomly located within predefined spatial constraints, forming a spatially structured point pattern that covered both littoral and pelagic zones. The spatial arrangement of stations was designed to capture major environmental gradients and to allow the joint analysis of spatial variability in physicochemical parameters and beta diversity.

A total of 31 georeferenced stations were established (Fig. 1b), following the recommendations of Legendre and Fortin (1989). This number of stations was considered sufficient to detect significant spatial autocorrelation, given the relatively low landscape heterogeneity of the lagoon (Delmeile 2009; Ver Hoef 2002). Stations were spaced approximately 500–700 m apart, with a higher density near the shore to better capture fine-scale spatial variability, and each sampling unit was defined by a circular area with a radius of 5–7 m. Four seasonal sampling campaigns were conducted in 2016, each lasting two to three days, to capture temporal variations. At each station, both phytoplankton community composition and environmental variables-including nutrient concentrations, chlorophyll-a, and physicochemical parameters-were recorded.

Phytoplankton sampling and preservation

To characterize diatom assemblages in the photic zone (including planktonic and tychoplanktonic taxa), quantitative sampling was conducted using a Niskin bottle. At each station, three 1-L subsamples were

collected at 0.5 m depth and pooled to obtain a homogenized composite sample (3 L), from which a 1.5-L aliquot was retained for laboratory analyses. During fieldwork, samples were kept chilled in an ice cooler and transported to the laboratory.

Upon arrival at the laboratory, the 1.5-L composite sample was subsampled. One fraction was filtered onto GF/F glass-fiber filters (47 mm; 0.7 µm nominal pore size) for chlorophyll-a determination, and the filtrate was used for dissolved nutrient analyses. The remaining fraction was preserved for quantitative phytoplankton counts.

Laboratory analyses

A subsample was filtered through Whatman™ GF/F filters (0.7 µm pore size) and the filtrate was used to quantify dissolved nutrients (NO_3^-, NO_2^-, NH_4^+, PO_4^{3-}, and SiO_2). Analyses were performed by standard colorimetric methods using a multiparameter bench photometer (HI 83200, Hanna Instruments®, Woonsocket, RI, USA). Nitrates (NO_3^-) were determined by the cadmium reduction method (EPA Method 353.2, U.S. Environmental Protection Agency, 1993), nitrites (NO_2^-) by the diazotization method (EPA Method 354.1, U.S. Environmental Protection Agency, 1971), ammonium (NH_4^+) by the Nessler method (ASTM D1426, ASTM International, 2021), phosphates (PO_4^{3-}) by the ascorbic acid method ((EPA Method 365.3, U.S. Environmental Protection Agency, 1978)), and silicates (SiO_2) by the heteropoly molybdenum blue method (ASTM D859, ASTM International, 2016). All procedures were performed following the manufacturer's instructions (Hanna Instruments, n.d.). Chlorophyll a was measured after filtration onto GF/F glass-fibre filters (0.7 µm), pigment extraction in 90% acetone for 24 h (cold, dark), and spectrophotometric readings at 665 and 750 nm before and after acidification following Lorenzen (1967), with chlorophyll a and pheopigments calculated from the corresponding equations (Rodier et al. 2016).

For quantitative phytoplankton (diatom) analyses, samples were immediately preserved with alkaline Lugol's iodine (final concentration 1% v/v) and stored in the dark at 4°C until analysis (≤ 3 months after sampling). Quantification followed the Utermöhl inverted-microscopy method (NF EN 15204): 10–50 mL (depending on turbidity) was allowed to settle in sedimentation chambers (26 mm internal diameter) for ≥ 24 h, and counts were performed at ×20 in randomly selected fields until ≥ 400 counting units (cells) were recorded per sample. Cell densities (ind. mL^{-1}) were calculated from the ratio of the total chamber area to the observed area, with the field diameter calibrated using a stage micrometer and ImageJ.

Taxa were identified using inverted and upright microscopes with standard floras (Hasle et al. 1995) and online databases (e.g., AlgaeBase, WoRMS, PlanktonNet, DiatomBase)

Statistics methods

To evaluate how diatom community composition varied across the lagoon and through the seasonal cycle, we applied a complementary set of beta-diversity, ordination, and geostatistical analyses. This workflow was designed to quantify spatial and temporal compositional change, identify the genera and stations contributing most to these patterns, and assess whether beta-diversity metrics exhibited spatial autocorrelation and interpretable spatial structure.

Beta-diversity analyses were conducted in R(R Core Team 2023) using adespatial on a sites × genera matrix. Presence–absence (0/1) data were used to quantify spatial beta diversity within each campaign (winter, spring, summer, fall) using Jaccard dissimilarity and its partitioning into turnover/replacement (repl) and nestedness/richness-difference (rich) components, following established partitioning frameworks (Baselga 2010, 2012; Podani and Schmera 2011; Carvalho et al. 2012 ; Legendre 2014) and implemented with beta.div.comp().

Because beta.div.comp() returns pairwise dissimilarities, repl and rich were summarized at the station level (mean across all pairwise comparisons per station within each campaign) to allow paired comparisons and regressions describing the balance between components across stations.

Temporal beta diversity between consecutive seasons (T1 vs T2) was assessed at each station using the Temporal Beta-diversity Index (TBI) (Legendre 2019), implemented with TBI(), which decomposes total change into losses (B) and gains (C). Paired comparisons and regressions were used to summarize whether temporal changes were dominated by losses vs gains and to describe the B–C relationship across stations; given potential spatial dependence among stations, these summaries were interpreted descriptively and complemented by geostatistical analyses.

Local and species contributions to beta diversity were computed using the “beta diversity = variance” framework (Legendre and De Cáceres 2013). Abundance data were Hellinger-transformed (Legendre and Gallagher 2001), and total beta diversity, LCBD and SCBD were obtained with beta.div(); LCBD was interpreted as station compositional uniqueness and SCBD as the contribution of genera to overall compositional heterogeneity.

Seasonal patterns were explored using Factor Analysis of Mixed Data (FAMD) (Pagès 2020 ; Legendre and Legendre1987), implemented in FactoMineR via Factoshiny (FAMDshiny), integrating environmental variables (Temp, pH, EC, DO, TDS, Sal, NO_3^-, NO_2^-, PO_4^{3-}, NH_4^+, SiO_2, Chl-a) together with selected beta-diversity metrics and the categorical factor season. Spatial structuring of beta-diversity metrics was assessed using global Moran’s I (Legendre and Legendre1987) and empirical variograms (nugget, sill and range); spatial interpolation used ordinary or universal kriging depending on the presence of spatial trends, with mapping in ArcGIS 10.8(ESRI 2019).

Results

Descriptive summary of environmental parameters

To provide environmental context for subsequent analyses, we summarized the main physicochemical variables across sampling stations and seasons (Table 1).

Table 1
Descriptive summary of physicochemical parameters

Variable	Mean	SE	Minimum	Median	Maximum
Temperature (°C)	20.277	0.468	13.000	19.105	29.400
pH	8.0157	0.0236	7.1600	8.0110	9.6150
Electrical conductivity (µS/cm)	269.6	20.1	44.8	240.2	542.0
Dissolved oxygen (mg/L)	6.676	0.195	3.450	6.635	10.630
Total dissolved solids (g/L)	44.486	0.934	26.100	48.650	54.120
Salinity (g/L)	31.783	0.253	27.300	31.800	35.500
Nitrate (NO_3^-; mg/L)	24.266	0.242	17.200	24.160	38.300
Nitrite (NO_2^-; mg/L)	1.068	0.136	0.070	0.220	6.500
Phosphate (PO_4^{3-}; mg/L)	1.558	0.114	0.100	1.100	5.200
Ammonium (NH_4^+; mg/L)	2.610	1.310	0.530	1.230	164.0
Silica (SiO_2; mg/L)	2.243	0.100	0.480	1.860	5.000
Chlorophyll-a (µg/L)	3.163	0.199	0.068	2.791	11.33

Descriptive statistics (Table 1) show that water temperature ranged from 13.0 to 29.4°C (mean = 20.3°C) and pH from 7.16 to 9.62 (median = 8.01). Salinity varied between 27.3 and 35.5 g/L (median = 31.8 g/L), with electrical conductivity and total dissolved solids also spanning wide ranges across observations. Nutrient concentrations are reported as ions (mg/L of NO_3^-, NO_2^-, PO_4^{3-} and NH_4^+): NO_3^- ranged from 17.2 to 38.3 mg/L, PO_4^{3-} from 0.10 to 5.20 mg/L, and NH_4^+ showed the largest spread (0.53–164 mg/L), indicating the occurrence of episodic peaks. Chlorophyll-a ranged from 0.068 to 11.33 µg/L (mean = 3.16 µg/L). Overall, these values provide descriptive context for subsequent analyses, but they are not used here to infer causal relationships or to classify conditions against external thresholds.

Taxonomic composition and ecological guilds

Table 2
Code list of diatom genera and assignment to ecological type (B:benthic, P:planktonic,T: tychoplanktonic).

Code	Genre	Type	Code	Genre	Type	Code	Genre	Type
Aula	*Aulacoseira*	**P**	Achs	*Achnanthes*	**B**	Diplo	*Diploneis*	**B**
Cheat	*Chaetoceros*	**P**	Achm	*Achnanthidium*	**B**	Ento	*Entomoneis*	**B**
Cyclo	*Cyclotella*	**P**	Amph	*Amphora*	**B**	Gram	*Grammatophora*	**B**
Guina	*Guinardia*	**P**	Clima	*Climacosphenia*	**B**	Licm	*Licmophora*	**B**
Melo	*Melosira*	**P**	Cocc	*Cocconeis*	**B**	Navi	*Navicula*	**B**
Odon	*Odontella*	**P**	Cymb	*Cymbella*	**B**	Pinn	*Pinnularia*	**B**
Para	*Paralia*	**P**	Diato	*Diatoma*	**B**	Rhop	*Rhopalodia*	**B**
Plagg	*Plagiogramma*	**B**	Lyre	*Lyrella*	**B**			
Pleu	*Pleurosigma*	**B**	Gyr	*Gyrosigma*	**B**			
Neid	*Neidium*	**B**	Frag	*Fragilaria*	**T**			
Rhoi	*Rhoicosphenia*	**B**	Syn	*Synedra*	**T**			
Staur	*Stauroneis*	**B**	Navi	*Navicula*	**T**			
Strii	*Striatella*	**B**	Amph	*Amphora*	**T**			
Suri	*Surirella*	**B**	Cymb	*Cymbella*	**T**			
Plagt	*Plagiotropis*	**B**	Nitz	*Nitzschia*	**B/T**			

Based on Utermöhl cell counts (cells L^{-1}), the quantitative inventory revealed a clear dominance of benthic pennate genera (e.g., *Navicula*, *Nitzschia, Amphora, Pinnularia, Diploneis, Surirella* and *Gyrosigma*), indicating an assemblage largely structured by the benthic compartment. Centric planktonic genera were also well represented (notably *Chaetoceros*, *Cyclotella, Aulacoseira, Guinardia, Odontella and Paralia*), supporting the presence of a persistent planktonic core. In addition, several tychoplanktonic taxa (e.g., *Fragilaria, Synedra* and some *Navicula, Nitzschia* and *Amphora*) contributed to a mixed assemblage consistent with benthic–pelagic coupling (Table 1).

Spatial Beta Diversity

Overall patterns and turnover-nestedness partitioning

To disentangle the mechanisms underlying spatial beta diversity across seasons, we partitioned total spatial dissimilarity into turnover/replacement (repl) and nestedness/richness-difference (rich) components (Table 2). Spatial beta diversity (D) and its components (turnover/replacement, repl; nestedness/richness-difference, rich) were computed for each season across the 31 sampling stations.

Table 3
Paired t-test comparing seasonal mean values of the spatial beta-diversity components corresponding to turnover/replacement (repl) and nestedness/richness-difference (rich) across sampling stations (n = 31).

Seasons	*repl (Mean ± SD)*	*rich (Mean ± SD)*	*Mean difference (repl − rich)*	*t-test*	*pvalue*
Fall	0.148 ± 0.044	0.120 ± 0.025	0.028	2.36	0.025*
Winter	0.293 ± 0.068	0.239 ± 0.070	0.055	2.35	0.026*
Spring	0.211 ± 0.078	0.159 ± 0.039	0.052	3.02	0.005**
Summer	0.157 ± 0.041	0.142 ± 0.040	0.014	1.19	0.242ns

*Significance codes: ns p ≥ 0.05; * p < 0.05; ** p < 0.01; *** p < 0.001.*

Paired t-tests comparing the spatial beta-diversity components (turnover/replacement, repl, vs nestedness/richness-difference, rich) across stations (n = 31) showed that repl was significantly higher than rich in fall (t = 2.36, p = 0.025), winter (t = 2.35, p = 0.026), and spring (t = 3.02, p = 0.005). The largest mean difference (repl − rich) was observed in winter (0.055), followed by spring (0.052) and fall (0.028). In summer, the difference between repl and rich was not significant (t = 1.19, p = 0.242).

We then assessed whether seasonal changes in the relationship between repl and rich were consistent across stations using regression models (Table 3).

Table 4
Seasonal regression models describing the relationship between spatial beta-diversity components: turnover/replacement (repl) and nestedness/richness-difference (rich) across sampling stations (n = 31).

Seasons	**Equation (rich vs repl)**	**R^2**	**F**	**p-value**
Fall	rich = 0.3040 − 1.304 × repl	54.1%	34.19	< 0.001**
Winter	rich = 0.4663 − 0.7272 × repl	56.1%	37.00	< 0.001**
Spring	rich = − 0.3084 + 6.479 × repl − 19.09 × $repl^2$	32.5%	6.73	0.004**
Summer	rich = 0.2047 − 0.3386 × repl	10.5%	3.42	0.075ns

*Significance codes: ns p ≥ 0.05; * p < 0.05; ** p < 0.01; *** p < 0.001.*

The regression models indicate a seasonal shift in the relationship between the two spatial beta-diversity components (repl vs rich). In fall and winter, rich decreased linearly with increasing repl, with relatively high explanatory power (R^2 ≈ 54–56%), suggesting that pairwise compositional differences were mainly associated with turnover/replacement rather than richness-difference. In spring, the relationship was best described by a significant quadratic model (R^2 = 32.5%), indicating a non-linear balance between components across stations. In summer, the relationship was weak and not significant (R^2 = 10.5%, p = 0.075), providing no robust evidence for a consistent repl–rich association.

Spatial structure, autocorrelation and dependence scales

To test whether spatial beta diversity and its components exhibited global spatial structure within each season, we computed Moran's I with associated p-values (Table 4).

Table 5
Seasonal values of Moran's I (IM) for spatial beta diversity (D) and its components (repl, turnover/replacement; rich, nestedness-/richness-difference), with associated p-values.

		Betadiversity component		
Seasons	I-Test	**repl**	**rich**	D
Fall	IM	0.66	0.35	0.66
	P-value	2.37E-11***	0.0016**	2.26E-11***
Winter	IM	0.244	0.33	0.415
	P-value	4.60E-03***	3.30E-04***	1.29E-05***
Spring	IM	0.45	0.25	0.43
	P-value	2.42E-06	0.0046	8.04E-06
Summer	IM	0.074	0.232	0.33
	P-value	0.154ns	0.00587**	0.00163**

*Significance codes: ns p ≥ 0.05; * p < 0.05; ** p < 0.01; *** p < 0.001.*

Moran's I indicated significant positive spatial autocorrelation for turnover/replacement (repl) and total spatial beta diversity (D) in fall, winter and spring (Table 4). For nestedness/richness-difference (rich), spatial autocorrelation was also significant in fall but weaker (Table 4). By contrast, summer showed no significant spatial autocorrelation for repl (IM = 0.074, p = 0.154), whereas rich (IM = 0.232, p < 0.01) and D (IM = 0.33, p < 0.01) remained significantly structured (Table 4).

To quantify the scale of spatial dependence, we fitted empirical variogram models and extracted nugget, sill and range parameters for D and its components (Table 5)

Table 6
Parameters of empirical variogram models (nugget, sill, range in m) for total spatial beta diversity (D) and its components (turnover/replacement, repl; nestedness/richness-difference, rich) across seasons.

Seasons	Betdiversity-component	Nugget	Sill	Range
Fall	**repl**	1.70E-04	7.00E-04	8.54E + 02
	rich	1.00E-04	1.40E-04	1.52E + 03
	D	0.00E + 00	5.00E-04	1.01E + 03
Winter	**repl**	6.60E-04	5.60E-04	1.96E + 03
	rich	8.60E-04	3.70E-04	9.04E + 02
	D	1.64E-04	2.40E-04	2.06E + 03
Spring	**repl**	2.10E-03	8.20E-04	8.54E + 02
	rich	3.50E-04	2.20E-04	2.87E + 03
	D	1.30E-03	1.70E-03	8.54E + 02
Summer	**repl**	1.20E-04	3.50E-04	1.60E + 03
	rich	3.00E-04	2.60E-04	2.87E + 03
	D	3.20E-04	1.60E-04	1.16E + 03

*Significance codes: ns p ≥ 0.05; * p < 0.05; ** p < 0.01; *** p < 0.001.*

Variogram models showed that spatial structure in beta diversity was distance-dependent, with ranges on the order of ~ 0.85–1.96 km for turnover/replacement (repl) and ~ 0.85–2.87 km for nestedness/richness-difference (rich) across seasons (Table 5). Total beta diversity (D) exhibited shorter spatial ranges in fall–winter (range = 1.01 km) but longer ranges in winter and spring (2.06–2.87 km) (Table 5). Nugget and sill values varied among seasons and components, suggesting seasonal differences in short-range variability (nugget) and in the magnitude of spatially structured variance (sill).

Seasonal maps of D, repl and rich were generated by kriging to highlight the spatial structure of beta-diversity components across the lagoon (Fig. 2).

The kriging maps (Fig. 4) are consistent with the spatial dependence detected by Moran's I and with the variogram ranges. Higher Moran's I values associated with short-to-intermediate ranges (notably for repl and D in fall and spring) correspond to more spatially contrasted patterns. In summer, the more homogeneous patterns are consistent with the lack of significant spatial autocorrelation for repl, while rich and D remain significantly structured, suggesting a comparatively more continuous (intermediate–longer range) spatial pattern for these metrics.

Contributions of taxa and sites to beta diversity

To identify the taxa and sites that contributed most to spatial compositional heterogeneity, we examined species (SCBD) and local (LCBD) contributions to beta diversity across seasons (Fig. 3).

SCBD revealed that a restricted set of taxa consistently drove spatial compositional heterogeneity within each season (Fig. 5a). In autumn, the strongest contributions were from *Paralia* (Para), *Aulacoseira* (Aula) and *Cymatopleura* (Cyma), whereas winter was dominated by *Paralia* (Para), *Nitzschia* (Nitz) and *Aulacoseira* (Aula). In spring, contributions peaked for *Plagiogramma* (Plagg), *Navicula* (Navi), *Chaetoceros* (Chaet) and *Rhopalodia* (Rho), while summer was mainly characterized by *Paralia* (Para), *Navicula* (Navi), *Plagiogramma* (Plagg) and *Aulacoseira* (Aula). Overall, only 3–5 taxa per season displayed elevated SCBD values, whereas most taxa contributed less than 0.05.

LCBD varied across stations and seasons (Fig. 5b), indicating that only a limited number of sites were consistently distinctive. The most distinctive stations were 8, 9 and 21 in autumn, and 23–24 in winter; in spring, higher LCBD values clustered in the central–eastern sector. In contrast, summer showed a more spatially diffuse pattern of elevated LCBD.

Environmental variables affecting spatial beta diversity

FAMD was used to explore seasonal structure by jointly ordinating environmental variables and spatial beta-diversity metrics (D, repl and rich), with Season included as the active qualitative factor (Fig. 4).

The first two dimensions explained 62.83% of the total variance (Dim1: 40.09%; Dim2: 22.73%). Dimension descriptions indicated that Season had a strong effect on both Dim1 and Dim2, as shown by one-way ANOVAs on axis scores (Dim1: $R^2 = 0.961$, $p < 0.001$; Dim2: $R^2 = 0.968$, $p < 0.001$), confirming a pronounced seasonal structuring of the ordination.

Dim1(Fig. 4b) captured the main seasonal gradient, separating summer from winter. Positive Dim 1 scores were associated with higher PO_4, NO_2, TDS, temperature, salinity and conductivity ($r = 0.69–0.87$; all $p < 0.001$), whereas negative scores were associated with higher dissolved oxygen ($r = -0.51$, $p < 0.001$) and higher spatial β-diversity values (rich: $r = -0.55$; repl: $r = -0.58$; D: $r = -0.73$; all $p < 0.001$). Consistently, summer showed strongly positive scores on Dim 1(Fig. 4a) (estimate = 3.86, $p \ll 0.001$), while winter showed strongly negative scores (estimate = − 3.57, $p \ll 0.001$).

Dim2 represented a secondary gradient primarily driven by autumn. Positive Dim 2 scores were linked to higher dissolved oxygen, conductivity and salinity (OD: $r = 0.78$; CE: $r = 0.69$; Sal: $r = 0.59$; all $p < 0.001$), while negative scores were associated with higher temperature ($r = -0.65$, $p < 0.001$) and lower values of D, repl and rich (D: $r = -0.54$; repl: $r = -0.42$; rich: $r = -0.42$; all $p < 0.001$). Season-level estimates supported this pattern, with fall contributing most strongly and positively to Dim2(Fig. 4a) (estimate = 3.44, $p \ll 0.001$), whereas spring, winter and summer were negative on this axis.

Temporal Beta Diversity

Asymmetry and coupling in species losses and gains

Paired comparisons of temporal beta-diversity components (losses, B, vs gains, C) revealed clear contrasts among seasonal transitions (Table 6).

Table 7
Paired t-tests comparing mean temporal beta-diversity components (losses B vs gains C) across seasonal transitions (n = 31 stations).

Seasonal transition	B (Mean ± SD)	C (Mean ± SD)	Mean difference (B − C)	t-value	p-value
Fall–Winter	0.3643 ± 0.2177	0.3666 ± 0.2550	−0.0024	−0.03	0.977 ns
Winter–Spring	0.0900 ± 0.0678	0.8172 ± 0.0857	−0.7272	−27.63	< 0.001***
Spring–Summer	0.6276 ± 0.2051	0.0542 ± 0.0627	0.5734	12.75	< 0.001***
Summer–Fall	0.4150 ± 0.3022	0.2188 ± 0.1286	0.1962	2.63	0.013*

*Significance codes: ns p ≥ 0.05; * p < 0.05; ** p < 0.01; *** p < 0.001.*

The fall–winter transition showed balanced turnover, with no detectable difference between losses (B) and gains (C) ($p = 0.977$). The winter–spring transition was clearly gain-dominated ($C > B$; $p < 0.001$), whereas spring–summer was loss-dominated ($B > C$; $p < 0.001$). The summer–fall transition also showed higher losses than gains ($B > C$; $p = 0.013$).

We further examined the coupling between losses and gains across stations using linear regressions (Table 7).

Table 8
Linear regression between temporal beta-diversity components (species losses B vs. species gains C) across seasonal transitions among sampling stations (n = 31).

Seasonal transition	Equation (B vs C)	R^2 (%)	F	p-value
Fall–Winter	B = 0.6342 − 0.7361C	74.4	84.08	< 0.001***
Winter–Spring	B = 0.6196 − 0.6481 C	67.1	59.02	< 0.001***
Spring–Summer	B = 0.7432 − 2.1310 C	42.4	21.37	< 0.001***
Summer–Fall	B = 0.8396 − 1.9400 C	68.2	62.09	< 0.001***

*Significance codes: ns p ≥ 0.05; * p < 0.05; ** p < 0.01; *** p < 0.001.*

Across all seasonal transitions, losses (B) and gains (C) were strongly and consistently negatively related across stations (all regressions $p < 0.001$), indicating that stations with higher gains tended to show lower losses and vice versa. This inverse B–C coupling was strongest in fall–winter ($R^2 = 74.4\%$) and remained high in winter–spring and summer–fall ($R^2 \approx 67–68\%$), but was weaker in spring–summer ($R^2 = 42.4\%$).

Spatial structure of temporal change

Global spatial autocorrelation of temporal beta diversity and its components was assessed for each seasonal transition using Moran's I (Table 8).

Table 9
Moran's I (IM) for temporal beta diversity and its components (B, losses; C, gains; D, total) across seasonal transitions, with associated p-values.

		Betadiversity-component		
Seasonal transitions	Test	B	C	D
Fall-Winter	IM	0.46765	0.364905	-0.082853
	P-value	6.34E-05	0.006E-03	0.722
Winter-Spring	IM	0.115884	0.004859	-0.105679
	P-value	0.294	0.791642	0.607
Spring-Summer	IM	0.005066	0.002293	0.11623
	P-value	0.787	0.783	0.289
Summer-Fall	IM	0.448199	0.285386	0.452801
	P-value	9.52E-05	0.0288	0.000934

*Significance codes: ns $p \geq 0.05$; * $p < 0.05$; ** $p < 0.01$; *** $p < 0.001$.*

Moran's I indicated significant positive spatial autocorrelation for temporal beta-diversity changes during the fall–winter and summer–fall transitions, whereas winter–spring and spring–summer showed no significant spatial autocorrelation. Specifically, fall–winter exhibited significant clustering for losses (B IM = 0.468, p = 6.34×10^{-5}) and gains (C; IM = 0.365, p = 0.006), while total change (D) was not significant (p = 0.722). Summer–fall showed significant clustering for losses (B; IM = 0.448, p = 9.52×10^{-5}), gains (C; IM = 0.285, p = 0.0288), and total change (D; IM = 0.453, p = 0.000934).

To further characterize the spatial structure and its scale, variogram models were fitted for temporal beta diversity and its components across transitions (Table 9).

Table 10
Variogram model parameters (nugget, sill, and range) for temporal beta diversity and its components (B, losses; C, gains; D, total) across seasonal transitions.

Seasons transition	Betdiv-component	Nugget	Sill	Range(m)
Fall-Winter	B	0.00E + 00	5.20E-02	9.93E + 02
	C	8.01E-05	8.00E-02	8.54E + 02
	D	7.71E-03	1.30E-02	9.08E + 02
Winter-Spring	B	3.80E-03	1.40E-03	1.77E + 03
	C	5.70E-03	2.30E-03	2.14E + 03
	D	1.80E-03	6.90E-04	1.39E + 03
Spring-Summer	B	4.06E-02	2.06E-03	2.87E + 03
	C	0.00E + 00	4.90E-03	9.35E + 02
	D	2.40E-02	7.10E-03	2.87E + 03
Summer-Fall	B	0.00E + 00	9.60E-02	9.84E + 02
	C	0.00E + 00	1.70E-02	8.54E + 02
	D	0.00E + 00	4.30E-02	9.30E + 02

Variogram parameters varied across seasonal transitions. Fall–winter and summer–fall showed short to intermediate spatial ranges (~ 850–990 m), with no nugget effect in summer–fall and a component-dependent nugget in fall–winter. Winter–spring displayed larger ranges (~ 1,390–2,140 m) and non-zero nugget effects for all components. Spring–summer showed mixed patterns, with short ranges for B and C (~ 935–953 m) but a much larger range for total change D (~ 2,870 m), and non-zero nugget effects for B and D.

To visualise the spatial organisation of temporal community change between seasons, we mapped TBI (Jaccard; D) and its components (B, losses; C, gains) using ordinary kriging (Fig. 5).

Spatial patterns in the kriged surfaces were consistent with Moran's I results (Table 9). Significant positive spatial autocorrelation in fall–winter and summer–fall indicated non-random clustering of temporal change, resulting in more patchy spatial structures for losses (B) and gains (C) (and for total change D in summer–fall). By contrast, winter–spring and spring–summer showed no significant global spatial autocorrelation, and the kriged maps displayed comparatively smoother spatial gradients.

Taxa affecting compositional heterogeneity over time

To identify which taxa most strongly drove compositional heterogeneity between consecutive seasons, we examined species contributions to beta diversity (SCBD) for each seasonal transition (Fig. 6).

SCBD patterns indicated marked shifts in the taxa contributing most to compositional heterogeneity across seasonal transitions (Fig. 6). The fall–winter and winter–spring transitions were driven primarilyby *Cymatopleura* (Cyma), *Plagiogramma* (Plagg), *Nitzschia* (Nitz) and *Achnanthes* (Achn), with *Rhoicosphenia* (Rho) also showing high contributions during winter–spring (max SCBD = 0.124). During spring–summer, the strongest contributors shifted to *Fragilaria* (Frag), *Neidium* (Neid), *Rhoicosphenia* (Rho), *Chaetoceros* (Chaet)and *Fragilaria* (Frag). The highest maximum SCBD was observed in summer–fall (0.129), dominated by *Plagiogramma* (Plagg), *Paralia* (Para) and *Cymatopleura* (Cyma), whereas the lowest maximum SCBD occurred in summer and fall (0.086).

Environmental variables affecting temporal beta diversity

To assess how temporal beta diversity (TBI; B losses, C gains, D total change) covaries with environmental conditions across seasonal transitions, we performed a FAMD on transition × station sampling units (Fig. 7).

The first two dimensions explained 59.43% of total variance (Dim 1: 40.15%; Dim 2: 19.29%), and the categorical factor Periods strongly structured both axes, as shown by one-way ANOVAs on axis scores (Dim 1: $R^2 = 0.952$, $p = 9.72\times10^{-79}$; Dim 2: $R^2 = 0.971$, $p = 4.80\times10^{-92}$).

Dim1(Fig. 7a) separated Summer–Fall (positive; estimate = 3.80) from Winter–Spring (negative; estimate = − 3.40) and, to a lesser extent, Fall–Winter (estimate = − 1.05). Positive Dim 1 (Fig. 7a) scores were associated with warmer and more nutrient-enriched/mineralised conditions (Temp r = 0.87, PO_4 r = 0.85, NO_2 r = 0.84, TDS r = 0.71, NO_3 r = 0.68, SiO_2 r = 0.64, Sal r = 0.54), and with higher losses (B; r = 0.45). Negative Dim 1 scores were associated with higher conductivity (CE; r = − 0.77), higher gains (C; r = − 0.72), higher dissolved oxygen (OD; r = − 0.70), and higher total temporal change (D; r = − 0.57).

Dim2(Fig. 7b) contrasted Fall–Winter (positive; estimate = 2.34) with Spring–Summer (negative; estimate = − 2.70), while Summer–Fall was slightly positive (estimate = 0.75). Positive Dim 2(Fig. 7b) scores were driven mainly by salinity (r = 0.80), dissolved oxygen (r = 0.62), conductivity (r = 0.60) and pH (r = 0.54), whereas negative scores were associated with higher temperature (r = − 0.32) and higher losses (B; r = − 0.33).

Discussion

This study confirms that a beta-diversity framework is useful for describing community assembly and diagnosing ecosystem change in lagoon environments. In El Mellah Lagoon, marked seasonality and strong within-lagoon heterogeneity coincide with pronounced spatial and temporal variation in diatom community composition (Figs. 3–4; Tables 3–5–7–9), consistent with the view that diatom beta diversity reflects both environmental gradients and spatial mechanisms in aquatic systems (Jamoneau et al. 2017).

Partitioning of spatial beta diversity shows that among-station dissimilarity is mainly driven by turnover/replacement (repl) rather than richness-difference (rich) during autumn, winter and spring, whereas the difference between repl and rich is not significant in summer (Table 3). This indicates that replacement processes dominate spatial differentiation during most of the year and that richness-related differences contribute more comparably in summer, supporting the idea that richness variation and turnover capture distinct mechanisms of community change (Hu et al. 2019). Seasonal regressions further show that the

repl–rich relationship shifts from strong linear coupling in autumn and winter to a non-linear pattern in spring and an absence of a clear association in summer (Table 4), suggesting that the balance between replacement-driven differentiation and richness-difference is season dependent.

Geostatistical analyses refine the interpretation of spatial structure by separating magnitude and configuration. Moran's I reveals significant positive spatial autocorrelation for repl and total dissimilarity (D) in autumn, winter and spring, whereas in summer repl shows no significant spatial autocorrelation while rich and D remain structured (Table 5). Variogram ranges in the order of 0.8–2.9 km for repl, rich and D confirm that beta-diversity components are spatially structured at sub-lagoon scales, with shorter ranges associated with more contrasted kriging maps (Table 6; Fig. 2). These patterns are consistent with studies showing that diatom beta diversity increases with spatial extent and can decrease under nutrient enrichment at broader scales, underscoring the influence of environmental context and scale on spatial heterogeneity (Leboucher et al. 2019; Dormann 2007; Rossi et al. 1992; Taibi et al. 2021)

The FAMD further supports a strong seasonal organisation of spatial patterns by ordinating stations along axes jointly structured by salinity, conductivity, nutrients, oxygen and beta-diversity metrics (Fig. 4). Dim 1 separates mainly summer from winter along a gradient of higher temperature, salinity and nutrients versus higher oxygen and higher D, repl and rich, while Dim 2 highlights autumn as a distinct configuration with elevated salinity, conductivity and dissolved oxygen and lower beta-diversity values (Fig. 4). This configuration is coherent with results from coastal wetlands where salinity gradients and environmental heterogeneity are reported as major drivers of diatom assemblage structure (Dalkıran and Zönülbil-Ünsal 2023). SCBD and LCBD analyses indicate that only a limited set of taxa with high SCBD and a subset of stations with high LCBD contribute disproportionately to spatial beta diversity (Fig. 3), in line with work showing that diatom beta diversity at multiple spatial scales can be effectively described by focusing on a reduced set of informative taxa and sites (Jyrkänkallio-Mikkola et al. 2015).

Temporal beta diversity (TBI) reveals strongly asymmetric seasonal transitions, indicating that compositional change among seasons is not uniform around the annual cycle (Table 7). The autumn–winter transition shows balanced change, with no detectable difference between losses (B) and gains (C), whereas winter–spring is clearly gain-dominated and both spring–summer and summer–autumn are loss-dominated (Table 7). This pattern is compatible with seasonal turnover described for planktonic diatoms in coastal bays, where distinct seasonal assemblages and sharp shifts in composition have been reported, highlighting that different parts of the year can be associated with either community expansion or contraction (Qi et al. 2015).

Across all transitions, losses and gains are strongly and negatively related among stations (Table 8), showing that stations with high gains tend to display low losses and vice versa. This systematic B–C trade-off indicates that temporal beta diversity arises from contrasting local modes of change within the same transition (replacement-like gains vs contraction-like losses), which matches conceptual frameworks that partition temporal beta diversity into extinction- and colonisation-related components whose relative dominance can vary through time (Tatsumi et al. 2021). In practical terms, the B–C relationship suggests that different lagoon sectors alternately act as sources (gain-dominated) or sinks (loss-dominated) of taxa along the seasonal cycle.

The spatial dimension of temporal change also differs among transitions. Moran's I indicates significant spatial autocorrelation for losses, gains and, in some cases, total temporal dissimilarity (D) in autumn–winter and summer–autumn, whereas winter–spring and spring–summer show no significant global spatial autocorrelation (Table 9). Variogram models confirm that the spatial range of temporal dependence is generally on the order of 0.8–2.1 km, with shorter ranges and low nuggets associated with more patchy kriging maps (Table 10; Fig. 5). These results suggest that some transitions (autumn–winter, summer–autumn) are characterized by spatial clusters of strong temporal change, while others (winter–spring, spring–summer) follow smoother spatial gradients, consistent with the idea that temporally varying environmental regimes structure temporal beta diversity in diatom assemblages (Wu et al. 2024 ; Griffiths 2024)

Species-level contributions indicate that different sets of taxa drive compositional heterogeneity between consecutive seasons (Fig. 6). High SCBD values for a small number of genera in each transition (e.g. *Cymatopleura, Plagiogramma, Nitzschia, Achnanthes, Fragilaria, Chaetoceros* and *Paralia*) show that temporal beta diversity is concentrated in a subset of strongly responsive taxa whose identity changes from one transition to another (Fig. 6). This concentration of contribution is in line with the expectation that temporal beta diversity can be dominated by environmentally sensitive or opportunistic taxa, while most genera remain relatively stable.

Finally, the FAMD integrating temporal beta diversity (B, C, D), environmental descriptors and the factor "Period" shows that transitions are clearly separated in the multivariate space by distinct combinations of environmental conditions and temporal change (Fig. 7). The first-dimension contrasts Summer–Autumn, associated with warmer and more nutrient-enriched, mineralised conditions and higher losses, with Winter–Spring, associated with cooler, more oxygenated waters and higher gains and total temporal change, whereas a second-dimension isolates Autumn–Winter with higher salinity, conductivity and dissolved oxygen (Fig. 7). These patterns support the view that no single environmental gradient explains all transitions and that the expression of temporal beta diversity depends on season-specific combinations of temperature, nutrients and hydrological conditions (Wu et al. 2022b). In this context, the empirically observed association between spatial and temporal beta diversity in phytoplankton (Zhang et al. 2017 Qiu and Cardinale 2020) and the documented differences in temporal dynamics across trophic contexts (Korhonen et al. 2013) provide a coherent framework for interpreting why only some transitions exhibit spatial clustering of temporal change and why gain- versus loss-dominated phases align with different environmental regimes.

Conclusion

This study illustrates that integrating spatial and temporal beta-diversity analyses can provide a detailed description of seasonal community change in a Mediterranean coastal lagoon. In El Mellah Lagoon, diatom beta-diversity patterns differed among seasons, with spatial turnover generally dominating over richness-difference and temporal transitions showing asymmetric balances between species losses and gains. Spatial and geostatistical analyses further indicated that some beta-diversity components are spatially clustered in specific seasons, whereas others follow smoother spatial gradients. A restricted set of taxa contributed disproportionately to compositional heterogeneity, and a subset of stations emerged as consistently distinctive, suggesting that beta-diversity metrics can help identify informative taxa and sites for

future monitoring. Overall, these results show that combining partitioned beta-diversity, contribution metrics and geostatistical tools is a useful approach to summarise spatio-temporal patterns of diatom community composition in lagoon systems. Future work linking these patterns to hydrodynamics, trait distributions and quantified pressure indicators would help to clarify underlying mechanisms and to test whether this framework is applicable to other transitional ecosystems.

Declarations

Ethical Statement

All field activities were conducted in accordance with national and institutional regulations for environmental research in Algeria. Sampling was performed under authorization from the El-Kala National Park authorities, and no protected or endangered species were collected or harmed during this study.

Funding Information

This work was supported by the *Ministère de l'Enseignement Supérieur et de la Recherche Scientifique (MESRS), Algeria*, through institutional funding provided to academic research staff.

Author Contribution

- **Dr. Samar Mohamed Faouzi (corresponding author)**: Study conception, supervision of all stages (sampling design, fieldwork, laboratory analyses, data processing, statistical modelling), manuscript writing and revision.
- **Dr. Bakaria Fatiha**: Participation in field sampling campaigns and microscopic laboratory analyses.
- **Dr. Larouci Nedjma**: Contribution to diatom identification and taxonomic validation.
- **Dr Abdallah Khadidja Wissal:** manuscript reviewing, and editorial support.
  All authors approved the final version of the manuscript.

Conflict of Interest

The authors declare no conflict of interest.

Acknowledgements

The authors thank the staff of El-Kala National Park for granting field access and providing logistical assistance. Special acknowledgment is extended to the **Laboratory of Marine Ecobiology and Coastal Environments, Badji Mokhtar Annaba University, Annaba, Algeria** and **Laboratory of Agriculture and Ecosystem Functioning Laboratory. Chadli Bendjedid El-Tarf University. El Tarf** for technical support during sample processing and analysis. We also gratefully acknowledge the *Ministère de l'Enseignement Supérieur et de la Recherche Scientifique (MESRS, Algeria)* for institutional encouragement and financial support.

References

1. Amara R, Rima E (2017) Fish assemblage structure in shallow waters of the Mellah Lagoon (Algeria): Seasonal and spatial distribution patterns and relation to environmental parameters. Acta Ichthyol Piscat 47(2):133–144. https://doi.org/10.3750/aiep/02080
2. ASTM International (2016) Standard test method for silica in water (ASTM D859-16). West Conshohocken, PA, United States
3. ASTM International (2021) Standard test methods for ammonia nitrogen in water (ASTM D1426-15(2021)e1). West Conshohocken, PA, United States
4. Baselga A (2010) Partitioning the turnover and nestedness components of beta diversity. Glob Ecol Biogeogr 19(1):134–143. https://doi.org/10.1111/j.1466-8238.2009.00490.x
5. Baselga A, Orme CDL (2012) betapart: an R package for the study of beta diversity. Methods Ecol Evol 3:808–812. https://doi.org/10.1111/j.2041-210X.2012.00224.x
6. Bellino A, Mangano MC, Baldantoni D, Russell BD, Mannino AM, Mazzola A, Vizzini S, Sarà G (2019) Seasonal patterns of biodiversity in Mediterranean coastal lagoons. Divers Distrib 25(10):1512–1526. https://doi.org/10.1111/ddi.12942
7. Carvalho JC, Cardoso P, Borges PAV, Schmera D, Podani J (2012) Measuring fractions of beta diversity and their relationships to nestedness: A theoretical and empirical comparison of novel approaches. Oikos 122(6):825–834. https://doi.org/10.1111/j.1600-0706.2012.20980.x
8. Dalkıran N, Zönülbil-Ünsal B (2023) Environmental heterogeneity and salinity gradient impacted the alpha and beta diversities of diatom assemblages in a coastal delta wetland. Water 15(19):3414. https://doi.org/10.3390/w15193414
9. Delmelle E (2009) Spatial sampling. In: The SAGE handbook of spatial analysis. SAGE Publications, pp 183–206. https://doi.org/10.4135/9780857020130.n10
10. Dormann CF (2007) Effects of incorporating spatial autocorrelation into the analysis of species distribution data. Glob Ecol Biogeogr 16(2):129–138. https://doi.org/10.1111/j.1466-8238.2006.00279.x
11. Draredja B (2007) Structure et fonctionnement d'un écosystème lagunaire méditerranéen : lagune Mellah (El Kala, Algérie). Ph.D. Thesis, University of Annaba, Algeria
12. Draredja B, Kara MH (2004) Caractères physico-chimiques de la lagune Mellah (Algérie nord-est). Rapp Comm Int Mer Méditerr 37:93
13. Draredja MA, Frihi H, Boualleg C, Gofart A, Abadie E, Laabir M (2019) Seasonal variations of phytoplankton community in relation to environmental factors in a protected meso-oligotrophic southern Mediterranean marine ecosystem (Mellah Lagoon, Algeria) with an emphasis on HAB species. Environ Monit Assess 191:603. https://doi.org/10.1007/s10661-019-7708-5
14. Draredja MA, Frihi H, Boualleg C, Abadie E, Laabir M (2020) Distribution of dinoflagellate cyst assemblages in recent sediments from a southern Mediterranean lagoon (Mellah, Algeria) with emphasis on toxic species. Environ Sci Pollut Res 27(20):25173–25185. https://doi.org/10.1007/s11356-020-08830-0
15. Environmental Systems Research Institute (ESRI) (2019) ArcGIS Desktop: Release 10.8 [Computer software]. Redlands, CA

16. European Committee for Standardization (2005) Water quality – Guidance standard for the routine sampling and preparation of benthic diatoms from rivers (EN 13946). Brussels
17. Gálvez Á, Castillo-Escrivà A, Magurran A, Alambiaga I, Bonilla F, Camacho A, García-Roger EM, Iepure S, Miralles-Lorenzo J, Monrós JS, Olmo C, Picazo A, Rojo C, Rueda J, Sasa M, Segura M, Armengol X, Mesquita-Joanes F (2023) Higher alpha and gamma, but not beta diversity in tropical than in Mediterranean temporary ponds: A multi-taxon spatiotemporal approach. Limnol Oceanogr 68(10):2402–2414. https://doi.org/10.1002/lno.12429
18. Griffiths J, Kelly MG, Juggins S, Yallop ML, Williams DM (2024) Diatom beta diversity across lake ecosystems: Linking environmental gradients to spatial patterns. Freshw Biol 69(2):245–260. https://doi.org/10.1111/fwb.14124
19. Guelorget O, Perthuisot JP, Lamy N, Lefebvre A (1982) Les lagunes littorales de la Méditerranée nord-occidentale : Caractérisation et évolution sédimentaire. Trav Lab Géol
20. Guelu C, Luk C, Ashton LA, Abbas S, Boyle MJW (2024) Beta diversity subcomponents of plant species turnover and nestedness reveal drivers of community assembly in a regenerating subtropical forest. Ecol Evol 14(9):e70233. https://doi.org/10.1002/ece3.70233
21. Hammill E, Hawkins CP, Greig HS, Kratina P, Shurin JB, Atwood TB (2018) Landscape heterogeneity strengthens the relationship between β-diversity and ecosystem function. Ecology 99(11):2467–2475. https://doi.org/10.1002/ecy.2492
22. Hanna Instruments (n.d.) HI 83200 multiparameter bench photometer for laboratories instruction manual [Instruction manual]
23. Hasle GR, Syvertsen EE, Steidinger KA, Tangen K (1995) Identifying marine diatoms and dinoflagellates (Tomas CR, ed). Academic Press
24. He Q, Zhang M, Wang J, Zhou S (2023) Local and regional drivers of beta diversity in aquatic ecosystems. Ecol Indic 148:110200. https://doi.org/10.1016/j.ecolind.2023.110200
25. He S, Qin C, Soininen J (2023) A flexible framework to assess patterns and drivers of beta diversity across spatial scales. Ecography 2024(2). https://doi.org/10.1111/ecog.06901
26. Heilpern SA, Weeks BC, Naeem S (2018) Predicting ecosystem vulnerability to biodiversity loss from community composition. Ecology 99(5):1099–1107. https://doi.org/10.1002/ecy.2219
27. Hu G, Wilson MC, Wu J, Yu J, Yu M (2019) Decoupling species richness variation and spatial turnover in beta diversity across a fragmented landscape. PeerJ 7:e6714. https://doi.org/10.7717/peerj.6714
28. Jamoneau A, Passy SI, Soininen J, Leboucher T, Tison-Rosebery J (2017) Beta diversity of diatom species and ecological guilds: Response to environmental and spatial mechanisms along the stream watercourse. Freshw Biol 63(1):62–73. https://doi.org/10.1111/fwb.12980
29. Jyrkänkallio-Mikkola J, Heino J, Soininen J (2015) Beta diversity of stream diatoms at two hierarchical spatial scales: Implications for biomonitoring. Freshw Biol 61(2):239–250. https://doi.org/10.1111/fwb.12697
30. Kherifi W, Hecini L, Bekiri F, Kherici-Bousnoubra H (2019) Faecal contamination of water in the Lake Mellah and its catchment area, north-eastern Algeria. J Water Land Dev 42(1):110–116. https://doi.org/10.2478/jwld-2019-0051

31. Korhonen JJ, Königs P, Soininen J (2013) Temporal variation of diatom assemblages in oligotrophic and eutrophic streams. Eur J Phycol 48(2):141–151. https://doi.org/10.1080/09670262.2013.779390
32. Larouci N, Samar F, Bensouilah M (2024) Spatial resilience of a lagoon ecosystem: The case of the El Mellah Lagoon (Northeastern Algeria). Egypt J Aquat Biol Fish 28(5):331–354. https://doi.org/10.21608/ejabf.2024.378877
33. Leboucher T, Bouchez A, Rimet F, Montuelle B (2019) Dispersal processes shape diatom metacommunity structure in river networks. Freshw Biol 64(4):761–776. https://doi.org/10.1111/fwb.13260
34. Leboucher T, Budnick WR, Passy SI, Boutry S, Jamoneau A, Soininen J, Vyverman W, Tison-Rosebery J (2019) Diatom diversity in streams increases with spatial scale and decreases with nutrient enrichment across regional to subcontinental scales. J Biogeogr 46(4):734–744. https://doi.org/10.1111/jbi.13517
35. Legendre P (2014) Interpreting the replacement and richness difference components of beta diversity. Glob Ecol Biogeogr 23(11):1324–1334. https://doi.org/10.1111/geb.12207
36. Legendre P (2019) A temporal beta-diversity index to identify sites that have changed in exceptional ways. Ecology 100(12):e02852. https://doi.org/10.1002/ecy.2852
37. Legendre P, De Cáceres M (2013) Beta diversity as the variance of community data: Dissimilarity coefficients and partitioning. Ecol Lett 16(8):951–963. https://doi.org/10.1111/ele.12141
38. Legendre P, Fortin MJ (1989) Spatial pattern and ecological analysis. Vegetatio 80(2):107–138. https://doi.org/10.1007/BF00048036
39. Legendre P, Gallagher ED (2001) Ecologically meaningful transformations for ordination of species data. Oecologia 129(2):271–280. https://doi.org/10.1007/s004420100716
40. Legendre P, Legendre L (1987) Numerical ecology. Elsevier
41. Legendre P, Legendre L (2012) Numerical ecology, 3rd English edn. Elsevier
42. Lorenzen CJ (1967) Determination of chlorophyll and pheopigments: Spectrophotometric equations. Limnol Oceanogr 12:343–346. http://dx.doi.org/10.4319/lo.1967.12.2.0343
43. Marion ZH, Fordyce JA, Fitzpatrick BM (2017) Pairwise beta diversity resolves an underappreciated source of confusion in calculating species turnover. Ecology 98(4):933–939. https://doi.org/10.1002/ecy.1753
44. Nakov T, Beaulieu JM, Alverson AJ (2019) Diatoms diversity and turnover despite widespread overlapping distributions. Nat Ecol Evol 3(4):486–490. https://doi.org/10.1038/s41559-019-0824-3
45. Pagès J (2020) Analyse factorielle multiple avec R. EDP Sciences. https://doi.org/10.1051/978-2-7598-1085-7
46. Pitacco V, Mistri M, Aleffi IF, Lardicci C, Prato S, Tagliapietra D, Munari C (2019) Spatial patterns of macrobenthic alpha and beta diversity at different scales in Italian transitional waters (central Mediterranean). Estuar Coast Shelf Sci 222:126–138. https://doi.org/10.1016/j.ecss.2019.04.026
47. Podani J, Schmera D (2011) A new conceptual and methodological framework for exploring and explaining pattern in presence–absence data. Oikos 120(11):1625–1638. https://doi.org/10.1111/j.1600-0706.2011.19451.x

48. Qi H, Xu Y, Hu X, Ma H, Xu H (2015) Seasonal shift in community pattern of planktonic diatoms and environmental drivers in Jiaozhou Bay, northern China. J Mar Biol Assoc U K 96(3):715–723. https://doi.org/10.1017/S0025315415000673
49. Qiu J, Cardinale BJ (2020) Scaling up biodiversity–ecosystem function relationships across space and time. Ecol Lett 23(4):751–763. https://doi.org/10.1111/ele.13472
50. R Core Team (2023) R: A language and environment for statistical computing. R Foundation for Statistical Computing, Vienna, Austria. https://www.R-project.org/
51. Rega M, Basset A, Stipcich M, Sabetta L (2023) Beta diversity indicators to support conservation priorities in Mediterranean transitional waters. Ecol Indic 150:110230. https://doi.org/10.1016/j.ecolind.2023.110230
52. Rodier J, Legube B, Merlet N (2016) L'analyse de l'eau, 10e edn. Dunod
53. Rolls RJ, Deane DC, Johnson SE, Heino J, Anderson MJ, Ellingsen KE (2023) Biotic homogenisation and differentiation as directional change in beta diversity: Synthesising driver–response relationships to develop conceptual models across ecosystems. Biol Rev 98(4):1388–1423. https://doi.org/10.1111/brv.12958
54. Rossi RE, Mulla DJ, Journel AG, Franz EH (1992) Geostatistical tools for modeling and interpreting ecological spatial dependence. Ecol Monogr 62(2):277–314. https://doi.org/10.2307/2937096
55. Soininen J, Heino J, Wang J (2017) A meta-analysis of nestedness and turnover components of beta diversity across organisms and ecosystems. Glob Ecol Biogeogr 27(1):96–109. https://doi.org/10.1111/geb.12660
56. Taibi H, Zaaboub N, Béjaoui B, Chapelle A, Aleya L (2021) Environmental drivers of spatial and temporal variability in Mediterranean lagoons: Implications for ecosystem management. Mar Pollut Bull 165:112111. https://doi.org/10.1016/j.marpolbul.2021.112111
57. Tatsumi S, Iritani R, Cadotte MW (2021) Temporal changes in spatial variation: Partitioning the extinction and colonisation components of beta diversity. Ecol Lett 24(5):1063–1072. https://doi.org/10.1111/ele.13720
58. Tatsumi S, Oksanen J, Svenning JC (2020) Beta diversity partitioning and species turnover along gradients of disturbance and productivity. Ecography 43(5):675–685. https://doi.org/10.1111/ecog.04936
59. U.S. Environmental Protection Agency (1971) Method 354.1: Determination of nitrite nitrogen by colorimetry (automated diazotization). In: Methods for the chemical analysis of water and wastes (MCAWW) (EPA/600/4-79/020). Cincinnati, OH
60. U.S. Environmental Protection Agency (1978) Method 365.3: Phosphorus, all forms (colorimetric, ascorbic acid, two reagent). In: Methods for the chemical analysis of water and wastes (MCAWW) (EPA/600/4-79/020). Cincinnati, OH
61. U.S. Environmental Protection Agency (1993) Method 353.2: Determination of nitrate-nitrite nitrogen by automated colorimetry (EPA/600/R-93/100). Cincinnati, OH
62. Utermöhl H (1958) Zur Vervollkommnung der quantitativen Phytoplankton-Methodik. Mitt Int Ver Theor Angew Limnol 9:1–38. https://doi.org/10.1080/05384680.1958.11904091

63. Ver Hoef J (2002) Sampling and geostatistics for spatial data. Écoscience 9(2):152–161. https://doi.org/10.1080/11956860.2002.11682701
64. Wu N, Dong X, Liu Y, Chen X, Cai Q (2022a) Stochastic dispersal processes drive diatom community assembly in riverine ecosystems. Sci Total Environ 806:150563. https://doi.org/10.1016/j.scitotenv.2021.150563
65. Wu N, Liu G, Qi X, Lin Z, Wang Y, Wang Y, Li Y, Oduro C, Khan S, Zhou S, Chu T (2024) Different facets of alpha and beta diversity of benthic diatoms along stream watercourse in a large near-natural catchment. Ecol Evol 14(6):e11577. https://doi.org/10.1002/ece3.11577
66. Wu N, Wang Y, Wang Y, Sun X, Faber C, Fohrer N (2022b) Environment regimes play an important role in structuring trait- and taxonomy-based temporal beta diversity of riverine diatoms. J Ecol 110(6):1442–1454. https://doi.org/10.1111/1365-2745.13859
67. Yao Z, Xin Y, Ma Z, Zhao L, Mu W, Guo J, Ali A (2024) Plant beta-turnover rather than nestedness shapes overall taxonomic and phylogenetic beta-diversity triggered by favorable spatial–environmental conditions in large-scale Chinese grasslands. Front Plant Sci 15:1285787. https://doi.org/10.3389/fpls.2024.1285787
68. Zhang M, Chen F, Shi X, Yang Z, Kong F (2017) Association between temporal and spatial beta diversity in phytoplankton. Ecography 41(8):1345–1356. https://doi.org/10.1111/ecog.03340

Figures

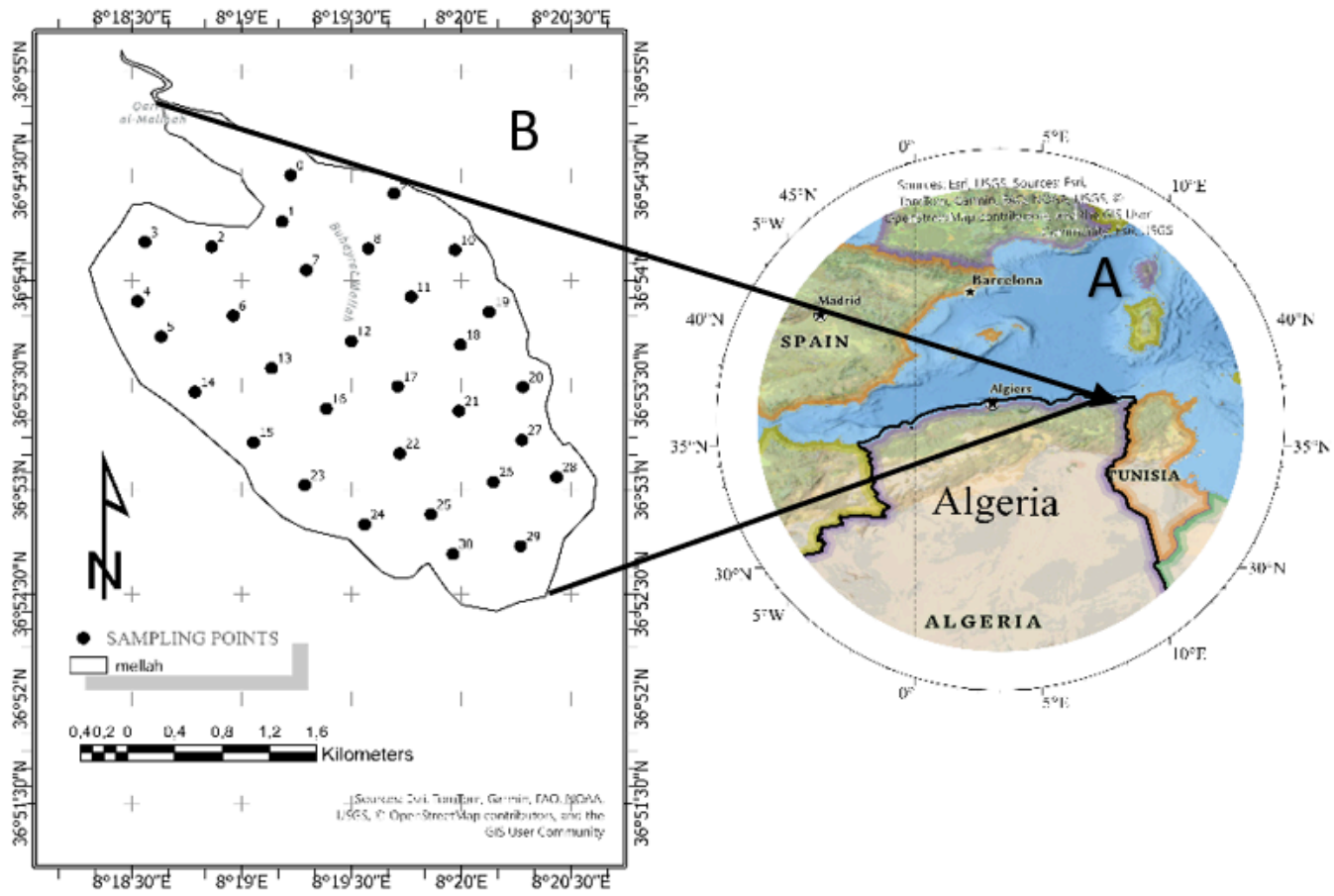


Figure 1

Study area (A) and sampling design (B)

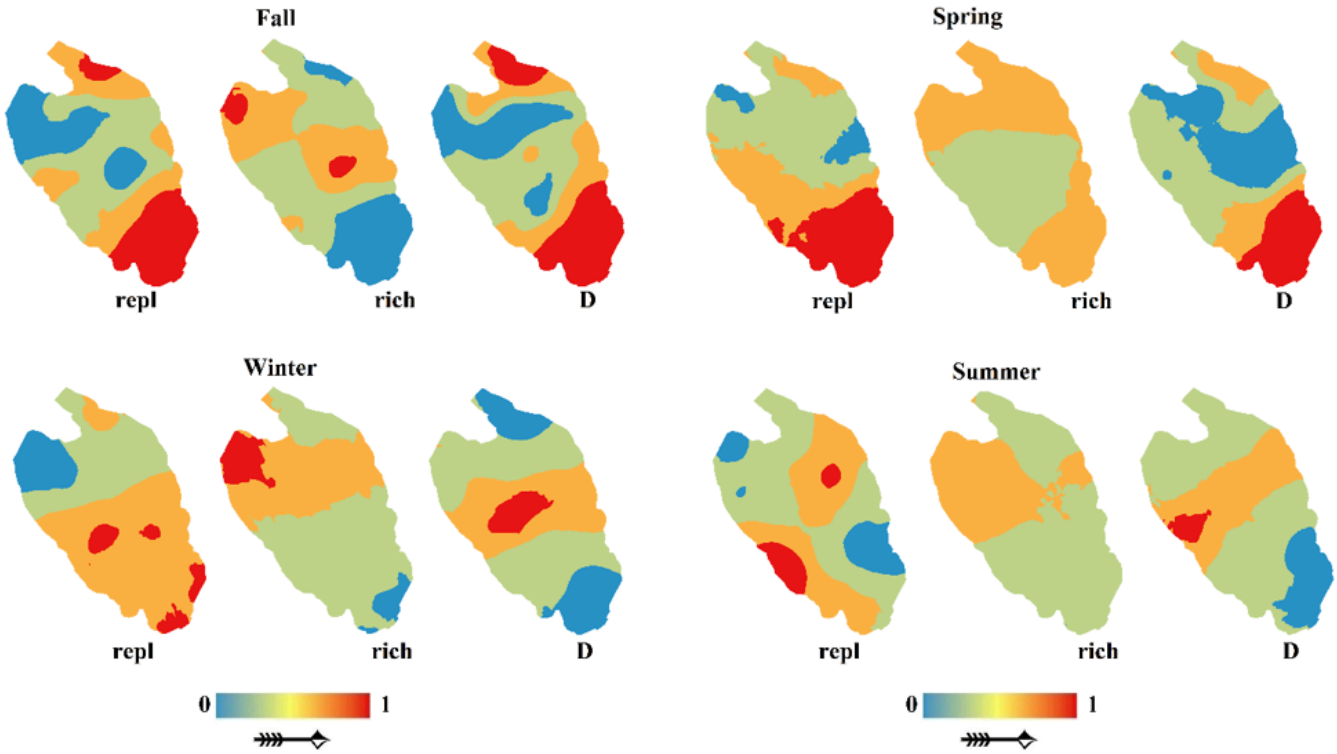


Figure 2

Kriging interpolation maps of spatial beta diversity (Jaccard dissimilarity; 0–1) across seasons, showing total spatial beta diversity (**D**) and its components: turnover/replacement (**repl**) and nestedness/richness-difference (**rich**). Warmer colors indicate higher dissimilarity. For each metric (repl, rich, and D), the same color scale (0–1) is used across seasons to enable direct inter-season comparisons.

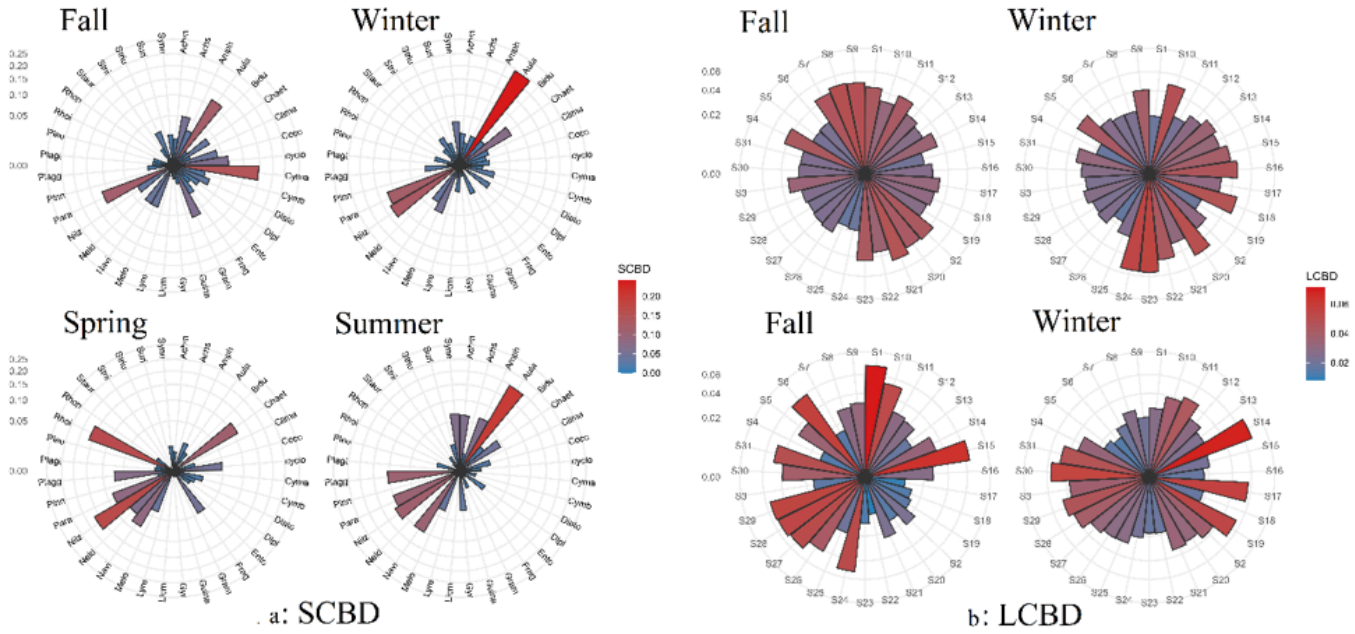


Figure 3

Rose diagrams showing (A) species contributions to beta diversity (SCBD) and (B) local contributions to beta diversity (LCBD) across seasons. Sn = station. Taxon abbreviations used in panel A are provided in Table 2.

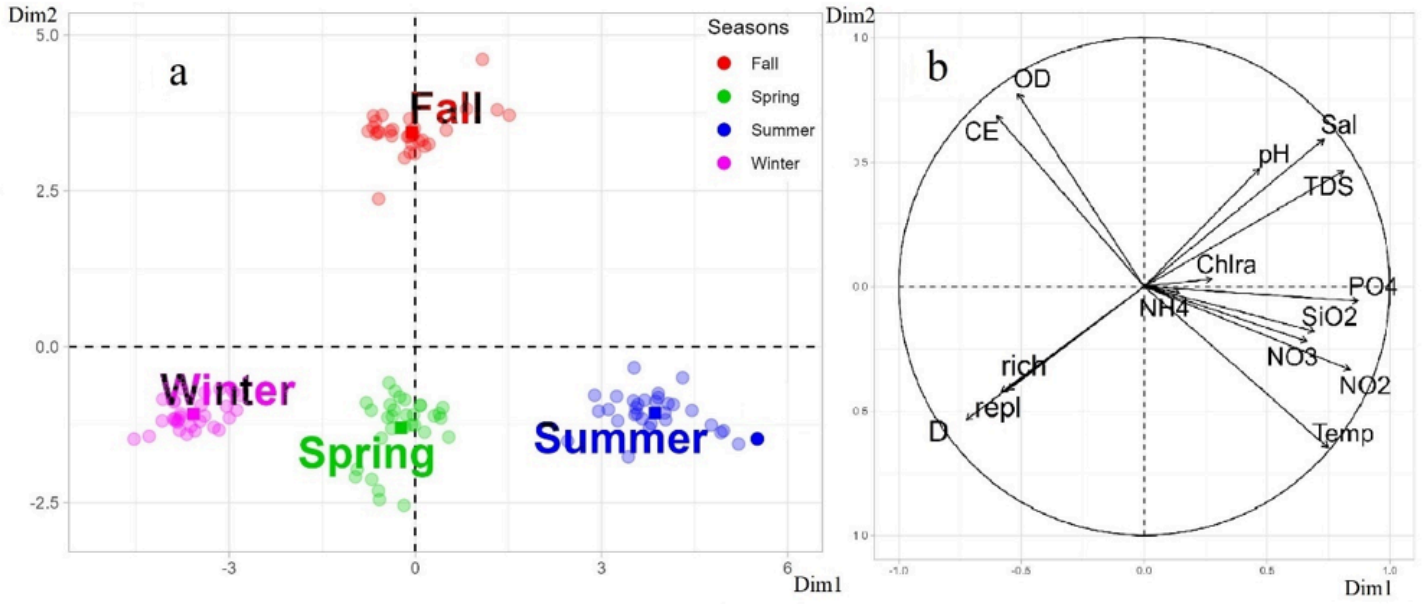


Figure 4

FAMD factorial plane (Dim 1–Dim 2) showing (a) the distribution of sampling units (season × station) and (b) the correlation circle of environmental variables and beta-diversity metrics.

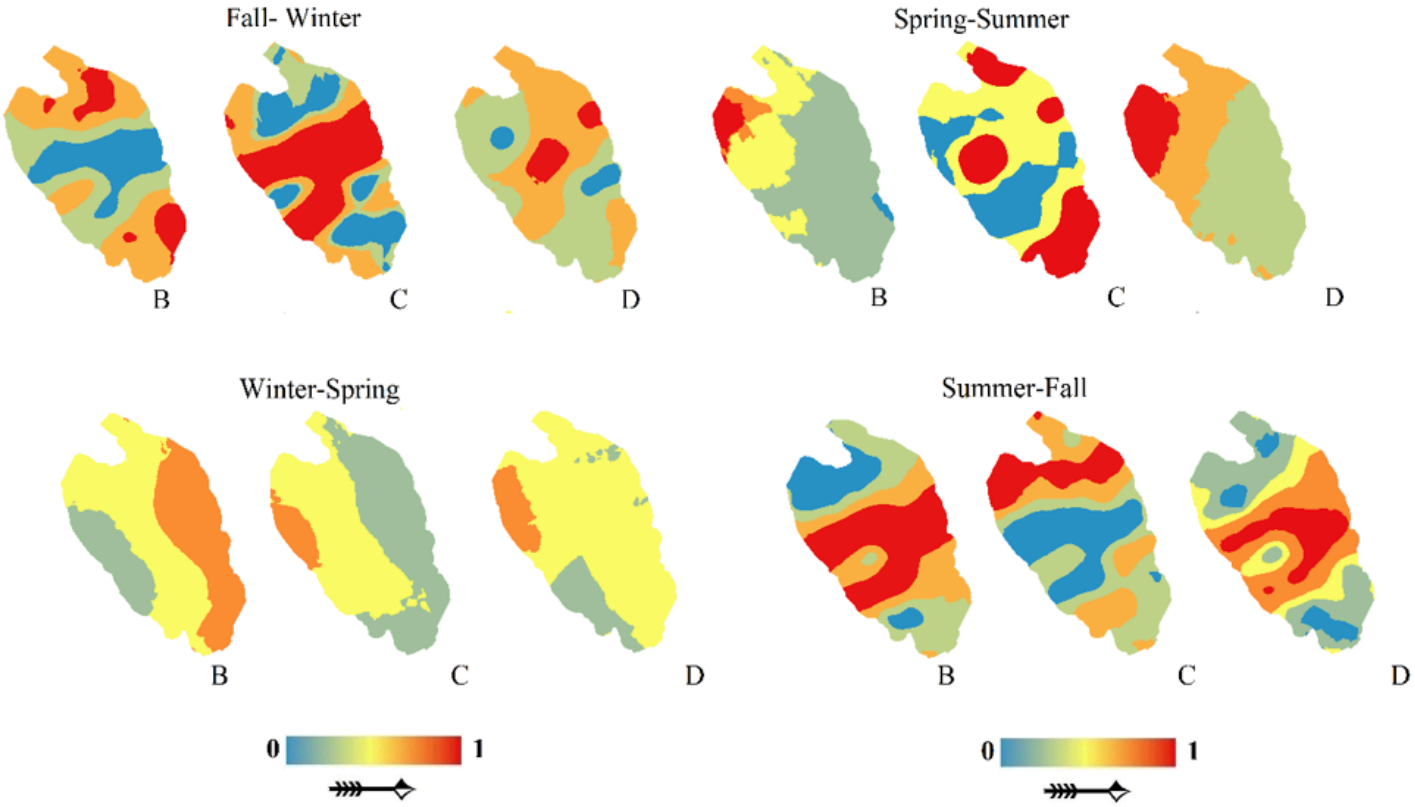


Figure 5

Ordinary kriging maps of temporal beta diversity (TBI; Jaccard dissimilarity; 0–1) across seasonal transitions, showing total temporal beta diversity (D) and its components: losses (B) and gains (C). Warmer colours indicate higher dissimilarity, and the same colour scale (0–1) is used across transitions to enable direct inter-season comparisons.

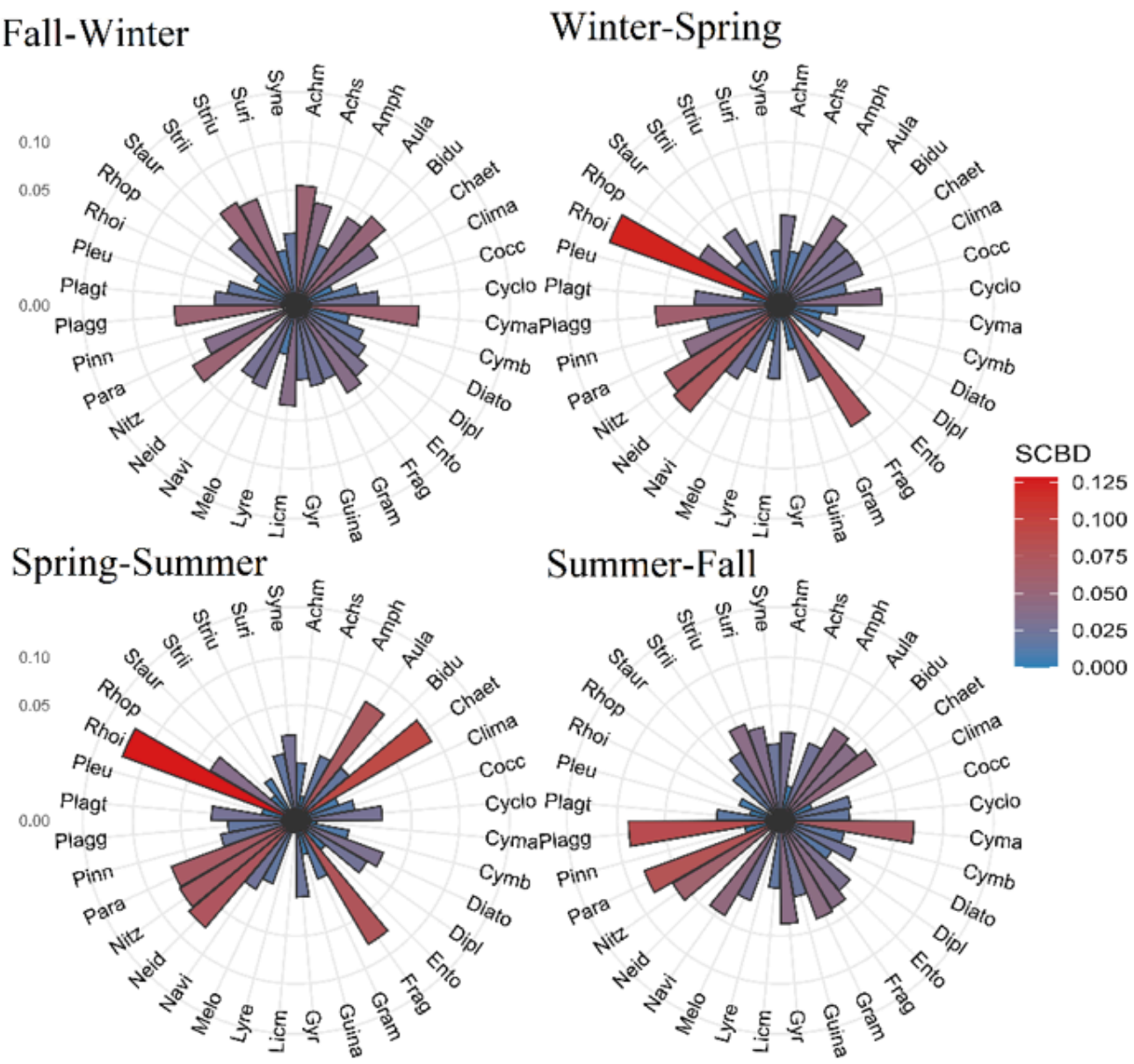


Figure 6

Rose diagrams showing species contributions to beta diversity (SCBD) for each seasonal transition. Taxon abbreviations are provided in Table 2.

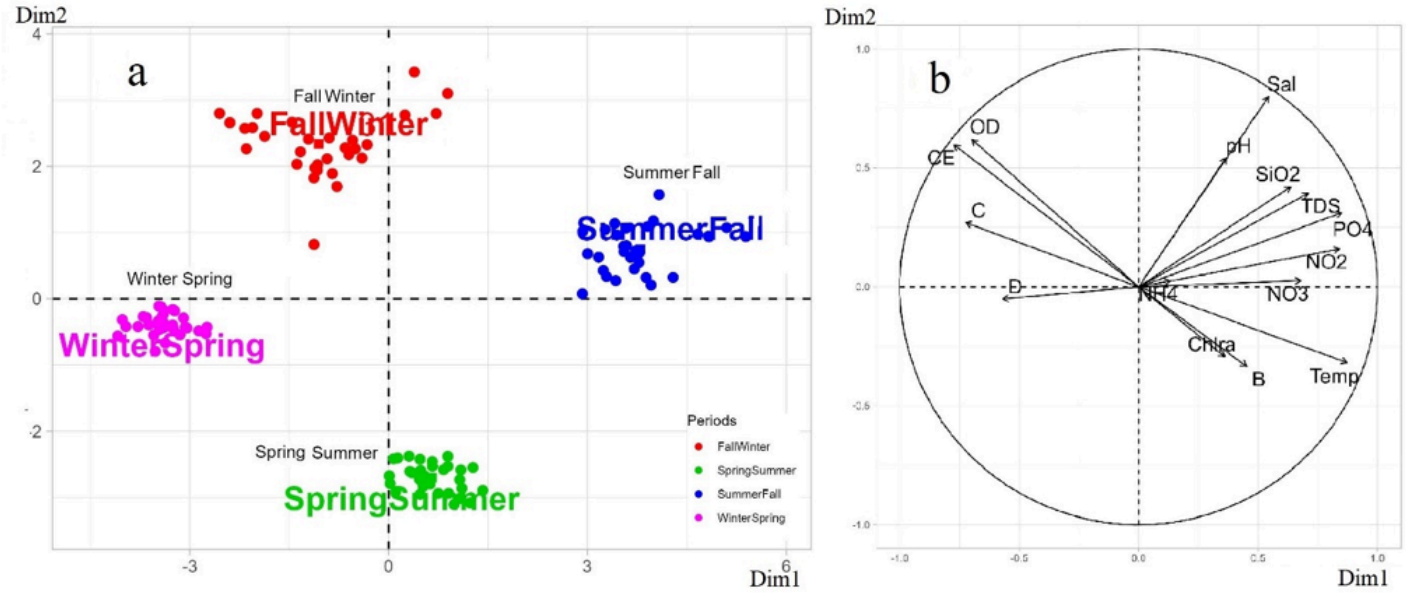


Figure 7

FAMD factorial plane (Dim 1–Dim 2) including temporal beta diversity (TBI), showing factor maps of (a) sampling units (transition × station) and (b) variables (TBI components and environmental descriptors).